UDC 621.318 https://doi.org/10.20998/2074-272X.2026.3.01

O. Belguet, R. Mehasni, A. Belounis, M. Ouili

Effects of friction on the efficiency of open gradient magnetic separation in dry granular materials

Introduction. *Magnetic separation is one of the most effective and widely used techniques for the purification and enrichment of materials. It plays a crucial role in mineral processing, recycling, and environmental applications, where the separation efficiency depends on both the magnetic field characteristics and the physical properties of the treated materials.* ***Problem.*** *A major limitation of existing studies is that the frictional drag force is often neglected in magnetic separation, although it can sometimes completely prevent the separation process.* ***Goal.*** *To estimate and experimentally verify the effect of frictional drag force on the performance and operational limits of open gradient magnetic separation (OGMS) under dry conditions.* ***Methodology.*** *An integrated analytical, numerical, and experimental approach was used. The granular medium was modeled as a complex fluid where friction acted as a drag force. The coupled magnetic and dynamic equations were solved using Finite Element (FE) – Runge–Kutta (RK4) methods, and results were validated experimentally with a permanent magnet drum separator.* ***Results.*** *To verify the obtained results experiments were carried out on samples of a mixture of sand and iron particles with different components sizes (iron particles and sand grains) in a permanent magnet drum separator. Limited to fine granulometries, the experiments carried out confirmed the results obtained theoretically.* ***Scientific novelty****. The study introduces a coupled FE–RK4 model that explicitly integrates the frictional drag force into the particle dynamic equations, enabling accurate prediction of trajectories and operational thresholds. This provides a realistic description of dry magnetic separation behavior, which has been largely overlooked in previous models of dry magnetic separation.* ***Practical value.*** *The findings provide engineers with a framework for optimizing dry OGMS performance. The developed model defines the threshold separating efficient from inhibited particle capture and clarifies how frictional drag controls the operational range of magnetic separators. These insights support improved design, process adjustment, and greater reliability in dry magnetic separation.* References 41, tables 7, figures 12.

Key words: **finite element method, fine particle, frictional drag force, granular material, magnetic field, magnetic separation, particle dynamics.**

Вступ*. Магнітна сепарація – один з найбільш ефективних і широко використовуваних методів очищення та збагачення матеріалів. Вона відіграє важливу роль у переробці мінералів, вторинній переробці та охороні навколишнього середовища, де ефективність поділу залежить як від характеристик магнітного поля, так і від фізичних властивостей оброблюваних матеріалів.* ***Проблема****. Основним обмеженням існуючих робіт є те, що сила тертя часто не враховується при магнітній сепарації, хоча іноді вона може заважати поділу.* ***Метою*** *роботи є оцінка та експериментальна перевірка впливу сили тертя на продуктивність та експлуатаційні межі відкритої градієнтної магнітної сепарації (OGMS) у сухих умовах.* ***Методика****. Використовувався інтегрований аналітичний, чисельний та експериментальний підхід. Гранульоване середовище моделювалося як складна рідина, де тертя діяло як сила опору. Зв'язані магнітні та динамічні рівняння розв'язувались з використанням методів скінченних елементів (FE) – Рунге–Кутта (RK4), а результати були експериментально підтверджені за допомогою барабанного сепаратора з постійними магнітами.* ***Результати****. Для перевірки отриманих результатів проведені експерименти на зразках суміші піску та частинок заліза з різними розмірами компонентів (частинки заліза та піщинки) у барабанному сепараторі з постійними магнітами. Експерименти з дрібнозернистим складом підтвердили теоретично одержані результати.* ***Наукова новизна****. У дослідженні представлена зв'язана модель FE–RK4, яка явно інтегрує силу тертя в рівняння динаміки частинок, що дозволяє точно прогнозувати траєкторії та робочі граничні значення. Це забезпечує реалістичний опис поведінки сухої магнітної сепарації, яка значною мірою ігнорувалась у попередніх моделях сухої магнітної сепарації.* ***Практична значимість****. Отримані результати надають інженерам основу оптимізації роботи сухих магнітних сепараторів. Розроблена модель визначає граничне значення, що розділяє ефективне і ускладнене захоплення частинок, і пояснює, як сила тертя контролює робочий діапазон магнітних сепараторів. Ці дані сприяють поліпшенню конструкції, коригування процесу та підвищенню надійності сухої магнітної сепарації.* Бібл. 41, табл. 7, рис. 12.

Ключові слова: **метод скінченних елементів, дрібнодисперсні частинки, сила тертя, гранульований матеріал, магнітне поле, магнітна сепарація, динаміка частинок.**

Introduction. Magnetic separation is a powerful process widely used in the mining industry notably for beneficiation and concentration of iron ores [1–5]. It is based on the application of magnetic field that allows the separation and recovery of the ferrous component in a desired site. The ore is initially extracted in form of rocks containing several minerals (iron, phosphor, zinc etc) with different concentrations. Before proceeding with magnetic separation which can be conducted in dry or wet ways [6–10], the constituting minerals are firstly dissociated by the grinding of the ore. The finer the grains, the better the dissociation.

Considering the water penury in arid regions on one hand and to avoid the pollution of the environment that can be caused by the ejection of water used in this process on the other hand, dry separation is favored in which permanent magnet drum separators are commonly used [11–13]. In these separators where open gradient magnetic field is used, the granular material to be treated is generally fed through a conveyor belt.

In fact, the separation process results from the action of applied forces that depend directly on the size of the constituent components (particles and grains). The fineness of the latter, which is advantageous for the dissociation of the material constituting minerals, can be a disadvantageous factor for the separation. In granular materials, the main forces acting on the particle to be separated are magnetic, gravity and frictional drag forces.

Numerous studies have investigated dry magnetic separation in granular media and various separators were designed without considering the frictional drag force that, in some cases, can have dominant effect [13–16].

The **goal of the work** is to estimate and experimentally verify the effect of frictional drag force on the performance and operational limits of open gradient magnetic separation (OGMS) under dry conditions.

The generator of the magnetic field is itself the capture element [14, 16–19].

The friction of solid object in non-cohesive granular media was studied in several works related to other problems. It was found that the domination of the frictional force depends on the object shape, velocity, depth and the medium specifications notably the packaging rate. To calculate the dynamics of the object, different models of the friction force were used, where the coefficients are determined experimentally according to the specifications of each problem [20–30].

Because in our application there are other conditions where the particles to be separated move randomly in a free-falling granular material (the material is not fed by conveyor belt but ejected vertically from a container under the effect of gravity), such models cannot be applied. Therefore, the moving granular material is modeled as a complex fluid in which the frictional force is approached to the fluid drag force for which an analytical model is used [31].

To estimate the effect of the frictional drag force on the separation efficiency and so on the use limits of the OGMS, we compared between the particle trajectories computed with and without considering such a force. For this purpose, and in order to take into account the coupling of the magnetic and particle dynamics phenomena in a study domain of complex geometry, a numerical resolution of the separation problem based on the coupling of Finite Element (FE) and Runge–Kutta (RK4) methods was carried out [16–19]. In such configurations, finite element methods are commonly employed for their robustness in dealing with irregular geometries and strongly coupled field–particle interactions [32, 33].

To verify the obtained results experiments were carried out on mixtures of sand and iron particles with different sizes and concentrations. For this purpose, a horizontal permanent magnets drum separator producing an open gradient magnetic field was used. The obtained results confirmed qualitatively what was found theoretically. They showed that the friction have significant effect that, in some cases of material granulometry and applied field, can even prevent the separation.

Modeling of the separation problem in dry granular medium. To separate the magnetic particles a static magnetic field is used. Because the permanent magnet drum is driven at a constant speed (Fig. 1), the spatial distribution of the magnetic field is computed at each rotation step by solving the equation given by [34]

$$\nabla\times\left(\frac{1}{\mu}\nabla\times\boldsymbol{A}\right)=\frac{1}{\mu}\nabla\times\boldsymbol{B}_r\,, \tag{1}$$

where $\boldsymbol{A}$ is the magnetic vector potential; $\boldsymbol{B}_r$ is the residual magnetic flux density of the magnets; μ is the magnetic permeability.

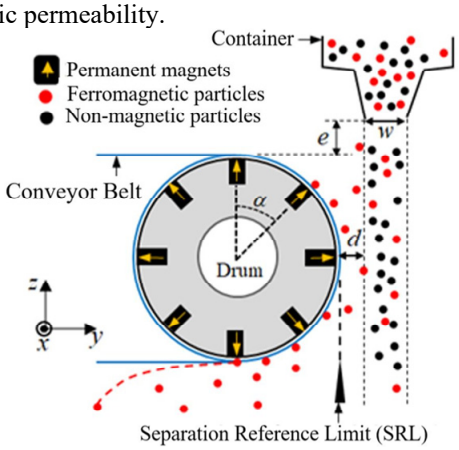

Fig. 1. 2D view of the considered dry drum separator

To compute the magnetic force applied on a magnetized particle, different approaches can be applied [35, 36]. In order to know the distribution of the magnetic force $\boldsymbol{F}_m$ and its nature in the environment of the separator, it is preferable to apply locally the formula given by [16, 18, 19, 37]:

$$\boldsymbol{F}_m=\mu_0\int_{V_p}(\boldsymbol{M}\cdot\nabla)\boldsymbol{H}\mathrm{d}V\,, \tag{2}$$

where $\boldsymbol{H}$ is the magnetic field strength; μ_0 is the magnetic permeability of vacuum; $\boldsymbol{M}$ is the particle magnetization; V_p is the particle volume.

The major disadvantage of (2) resides in its high sensitivity to the quality of the FE meshing of the study domain. The existence of FEs of bad quality can lead to singularities which generate significant errors. Such errors may significantly propagate during the computation process, particularly when successive spatial gradients are evaluated. For this reason, and given that the particles are rigid bodies, the Maxwell stress tensor method is applied. For an elementary surface $\mathrm{d}\boldsymbol{\Gamma}$ of the rigid particle, the force is given by [36]

$$\mathrm{d}\boldsymbol{F}_m=-\frac{1}{2}\mu_0\boldsymbol{H}^2\mathrm{d}\boldsymbol{\Gamma}+\mu_0(\boldsymbol{H}\cdot\mathrm{d}\boldsymbol{\Gamma})\boldsymbol{H}\,, \tag{3}$$

where $\mathrm{d}\boldsymbol{\Gamma}=\mathrm{d}\Gamma\boldsymbol{n}$, where $\boldsymbol{n}$ is the unitary vector normal to the surface of the particle body.

When the particle displaces in the granular medium, it enters in collision with the medium grains. Such collision results in a drag force that prevents its motion. To take into account this effect in the study of the particle dynamics, the granular medium is considered as a complex fluid for which the drag force $\boldsymbol{f}_D$ is approached analytically by [31]

$$\boldsymbol{f}_d=3\pi\eta_g D_p\boldsymbol{v}_{rel}\left(1+0.15R_e^{\,0.687}\right), \tag{4}$$

where η_g is the granular medium viscosity; D_p is the particle diameter, $\boldsymbol{v}_{rel}$ is the relative velocity between the particle and the medium; R_e is the Reynolds number of the particle.

The Reynolds number of the particle is given by [31]

$$R_e=\rho_e|v_{rel}|D_p/\eta_g\,, \tag{5}$$

where ρ_e is the effective density of the granular material; $\rho_e=\rho_s\cdot\varphi$, where ρ_s is the mass density of medium grains; φ is the packing fraction of the granular medium.

To distinguish the effect of the granular drag force on the particle behavior, it is necessary to study its motion without considering such a medium. In this case, one of the acting forces that merits to be considered is the drag force of air (fluid) given by [14]

$$\boldsymbol{f}_D=\frac{1}{2}A_p\rho_a C_D|\boldsymbol{v}_{rel}|\boldsymbol{v}_{rel}\,, \tag{6}$$

where A_p is the surface of the particle; ρ_a is air density; $\boldsymbol{v}_{rel}$ is the relative velocity between the particle and air (continuum phase); $C_d=24\left(1+0.15R_e^{\,0.687}\right)/R_e$ is the coefficient of drag of the particle. The Reynolds number is given by the following formula [14]

$$R_e=\rho_a|v_{rel}|D_p/\eta\,, \tag{7}$$

here η is the fluid (air) viscosity.

The other significant force applied on the particle is the gravitational force:

$$\boldsymbol{f}_g=m_p\boldsymbol{g}\,, \tag{8}$$

where $\boldsymbol{g}$ is the gravity acceleration; m_p is the particle mass.

According to the 2nd Newton's law, the computation of the particle motion requires the resolution of the dynamic equation given by [16–19],

$$m_p\frac{\mathrm{d}\boldsymbol{v}_p}{\mathrm{d}t}=\boldsymbol{f}_g+\boldsymbol{f}_D+\boldsymbol{F}_m\,, \tag{9}$$

here $\boldsymbol{v}_p$ is the particle velocity.

Resolution method and obtained results. To solve the separation problem, we have coupled the FE and RK4 numerical methods. Before proceeding to such a resolution, we firstly verified the accuracy of the magnetic modeling equations and the reliability of the developed FE computing tools. Such verification was based on the computation of the distributions of the magnetic field and force in the environment of the drum.

Applied magnetic field and generated force. To compute the distribution of the magnetic field in the geometrically complex domain, a 3D FE program was developed and used as in [38, 39]. To facilitate the interpretation and understanding of the results, we considered the case where the drum is static. The resolution of (1) and the exploitation of (2) for a drum of diameter D_d=0.1 m with 8 identical NdFeB magnets of B_r=1.1 T, cross sectional area S_M=0.01×0.012 m^2 and depth d_M=0.1 m arranged periodically with a spacing angle α=45° (see Fig. 1) have given the results presented in Fig. 2. Figure 2,*a* shows a periodic distribution of the magnetic vector potential that corresponds exactly to the chosen magnets polarity and arrangement; Fig. 2,*b* shows that a field of attractive magnetic force is obtained around the drum (to obtain the zoom, we presented only the force vectors in elements located out of the circle of radius 8·10^{-2} m).

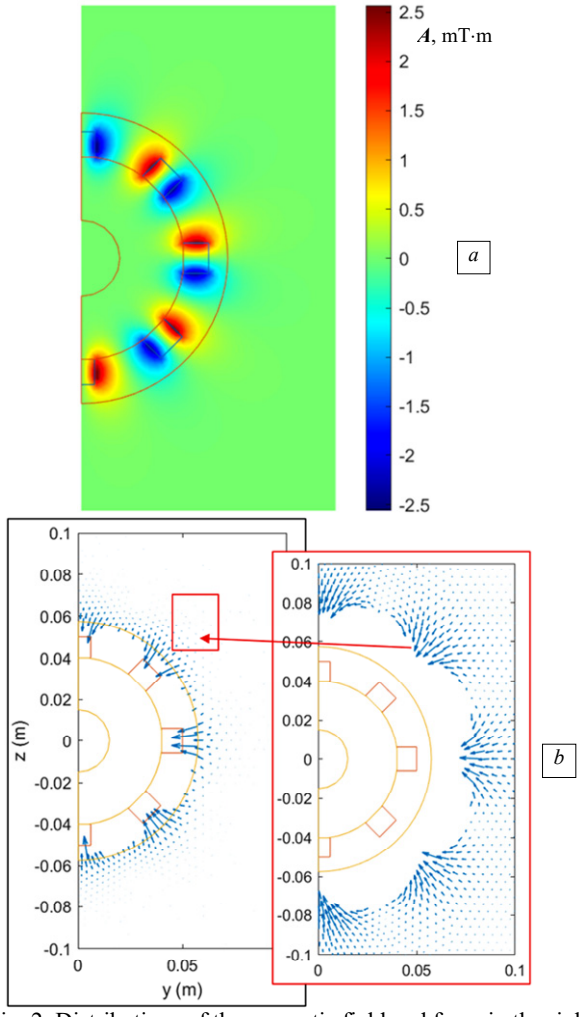

Fig. 2. Distributions of the magnetic field and force in the right side of the drum (plane (y, z)): *a* – magnetic vector potential; *b* – magnetic force density

To know quantitatively the specifications of the spatial distribution of the generated magnetic force, we computed the variations of its components following the 3 space directions x, y, z represented respectively by line 1 (x, D_d/2+75·10^{-4} m, 0), line 2 (0, y>D_d/2+75·10^{-4} m, 0) and line 3 (0, D_d/2+75·10^{-4} m, z) (see Fig. 3).

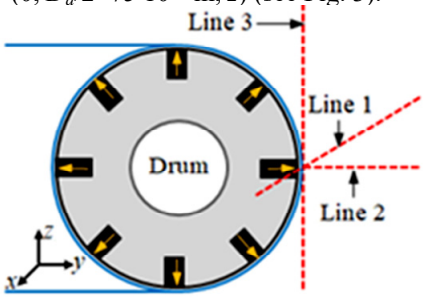

Fig. 3. Chosen lines for the representation of the variations of the magnetic force according to the 3 space directions respectively x, y, z

For the shown position of the drum magnets, we obtained the results presented in Fig. 4. Figure 4,*a* shows that along the length of line 2, only the component F_{my} can have effect. It is high near the drum surface and decreases sharply when we move away from it. Along the length of line 3, F_{mx} is negligible and only the components F_{my} and F_{mz} can have effect (see Fig. 4,*b*). The domination of each component depends on the evaluation position in relation to the magnets. Figure 4,*c* shows that on line 1, except weak effect of the component F_{mx} at the drum edges, there is a clear domination with quasi homogeneity of F_{my} along the length of the magnet.

When we move along the perimeter of the drum, we find the same result for F_{mx} with a decreasing of F_{my} and increasing of F_{mz}. The two components can have the same value near the immediately following magnets. At the lowest and highest magnets, it is F_{mz} that becomes dominant.

In absence of significant effect of the F_{mx} component and due to the quasi homogeneity of F_{my} and F_{mz} along the depth of the magnets, no considerable deflection of the particles according to the x direction can happen and the separation can occur indifferently along the depth of the separator. In these conditions, a 2D study of the separation problem in the plane (y, z) can sufficiently provide all information about the separation performance.

To compute the magnetic force applied on a magnetic particle, we used (3). Applied on the particle external surface, such a model permits the reduction of calculation errors linked to the quality of the meshing. For a cylindrical particle with a shape closer to a sphere of relative magnetic permeability μ_r=115, diameter D_p=1.6·mm and height h_p=1.6·mm located at the position shown in Fig. 5,*a*, we obtained the distribution of the force density presented in Fig. 5,*b*. The latter shows attractive elementary forces applied on the particle side opposite to the drum and repulsive elementary forces applied on its rear side but a resulting force oriented towards the drum. To verify the obtained force, we recalculated the force by applying (2), which has given for the same computing conditions the distribution of the force density presented in Fig. 5,*c*.

In Fig. 5,*c* the force is zero inside the particle, what we see inside the particle are the central points of the elements, where vectors of the elementary forces are computed and presented. The quantitative comparison between the results obtained by (2) and (3) has shown that the attractive resulting force is perfectly the same in terms of value and direction.

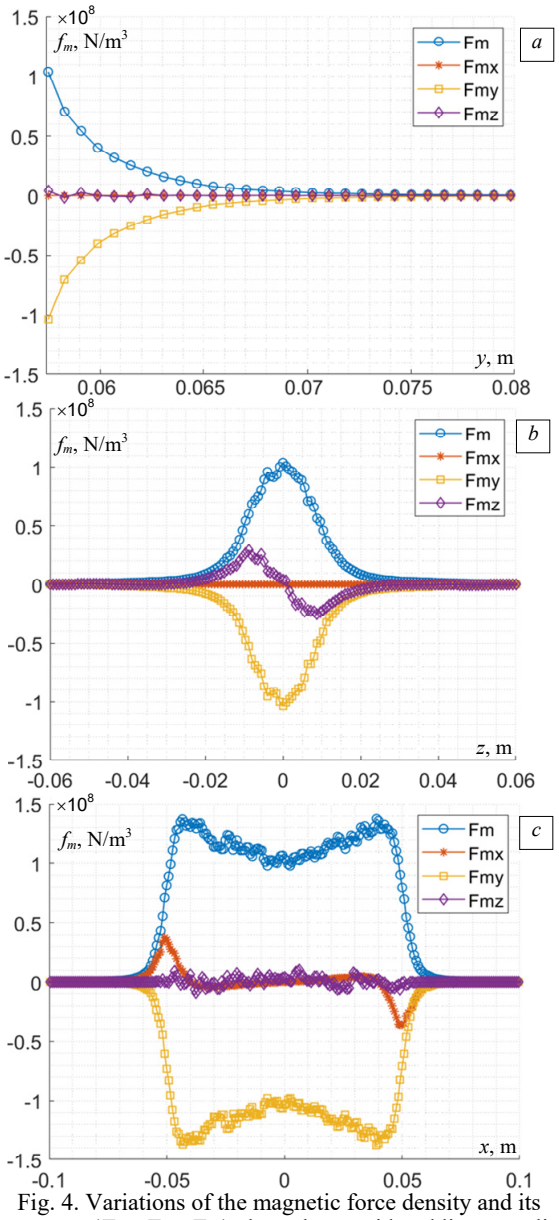

Fig. 4. Variations of the magnetic force density and its components (F_{mx}, F_{my}, F_{mz}) along the considered lines: *a* – line 2 (*y* direction); *b* – line 3 (*z* direction); *c* – line 1 (*x* direction)

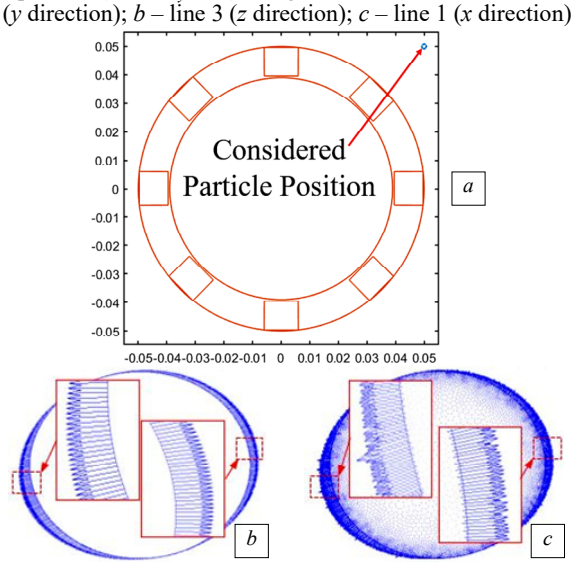

Fig. 5. Distribution of the magnetic force applied on a cylindrical particle of radius D_p=1.6 mm, height h_p=1.6 mm, μ_r=115 for a given position in respect to the drum: *a* – particle position; *b* – Maxwell stress tensor method; *c* – field gradient method

To consolidate our verification on one hand and to show that the force is globally attractive whatever the particle position on the other hand, we compared in Fig. 6 between the resulting components of the force obtained with (2) and (3) for different positions of the particle in respect to the drum. Such a comparison shows that the results are perfectly the same. Both the components of the global force are negative which means that they work to attract the particle towards the drum.

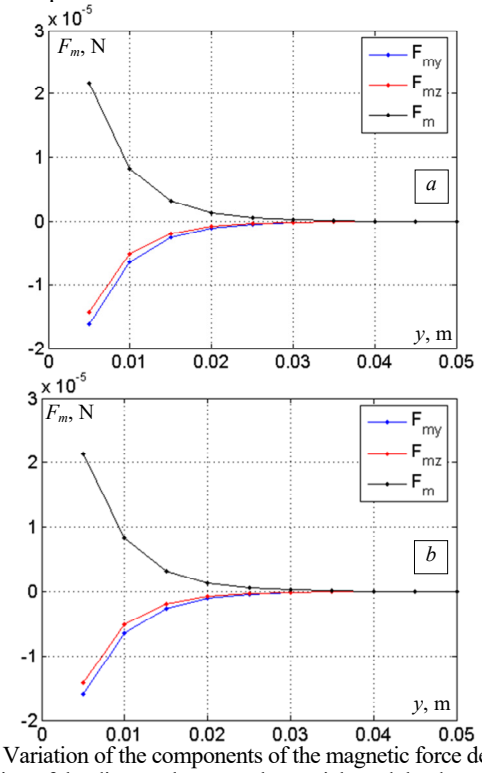

Fig. 6. Variation of the components of the magnetic force density as a function of the distance between the particle and the drum surface: *a* – Maxwell stress tensor method; *b* – field gradient method

Particle trajectory. To compute the particle trajectory that provides all information on its separation, we solved (9) where the particle body is taken into account (geometry and magnetic permeability). To permit the distinguishing of any effect of the granular frictional drag force on the separation, we firstly computed the particle trajectories without considering the granular medium. In this case, magnetic, gravitational and air drag forces modeled by (3), (6) and (8) respectively were taken into account. For ferromagnetic particles of diameters $7\cdot10^{-5}$ m < D_p < 10^{-2} m, height $h_p = D_p$, mass density ρ_p = 7874 kg/m^3, μ_r = 115, g = 9.81 m/s^2, we obtained for the particle initial positions of Table 1, the trajectories presented in Fig. 7.

Table 1

Considered particle initial positions

Particle number	Position *y*, m	Position *z*, m
1	$5.25\cdot10^{-2}$	$9\cdot10^{-2}$
2	$5.75\cdot10^{-2}$	$9\cdot10^{-2}$
3	$6.25\cdot10^{-2}$	$9\cdot10^{-2}$
4	$6.75\cdot10^{-2}$	$9\cdot10^{-2}$

Figure 7 shows that in absence of the granular frictional drag force, the capture occurs from a distance y_0 = $1.25\cdot10^{-2}$ m from the drum surface. Particles initially situated at the same position are almost captured at the same site, which means that for this range of particles, the particle size has no effect on the capture zone. On the contrary, the computed separation times (except the singular values

written in bold) presented in Table 2 show that for a given initial position, the particle of higher size is captured faster.

Table 2

Capture time of the separated particles without considering the granular frictional drag force

Particle diameter D_p ($\times 10^{-6}$ m)	Particle capture time, s		
	1	2	3
70	0.1190	**0.1278**	0.1422
150	0.1187	0.1280	**0.1410**
300	0.1186	0.1278	**0.1415**
800	0.1184	0.1278	0.1417
1500	0.1181	0.1277	0.1416
3000	0.1175	0.1273	0.1411
6000	0.1161	0.1262	0.1394
10000	0.1137	0.1239	0.1364

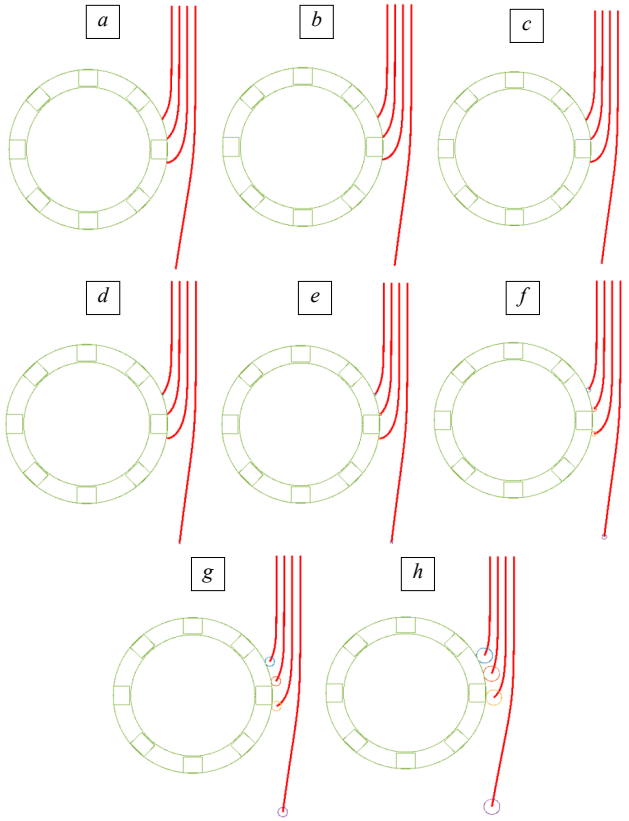

Fig. 7. Particle trajectories obtained for different particle sizes without considering the granular drag force: *a*) D_p=70·10^{-6} m; *b*) D_p=150·10^{-6} m; *c*) D_p=300·10^{-6} m; *d*) D_p=800·10^{-6} m; *e*) D_p=1500·10^{-6} m; *f*) D_p=3000·10^{-6} m; *g*) D_p=6000·10^{-6} m; *h*) D_p=10000·10^{-6} m

To estimate the effect of the granular frictional drag force on the separation, we recalculated the trajectories considering that the particles are included in a granular medium (sand) with homogeneous grains with a packing fraction φ=0.41 [40]. For the same previous computing conditions, we obtained the results presented in Fig. 8.

Figure 8 shows that the particles of diameter less than 300·10^{-6} m are not separated. Separation begins to occur for larger diameter particles initially falling very close to the drum (distance $y \leq 0.25 \cdot 10^{-2}$ m from the surface of the drum). We see also that the separation improves significantly with the increase in particle size. Unlike the previous case where the particle falls in air, in a granular medium, the size of the particle has considerable influence on the capture site.

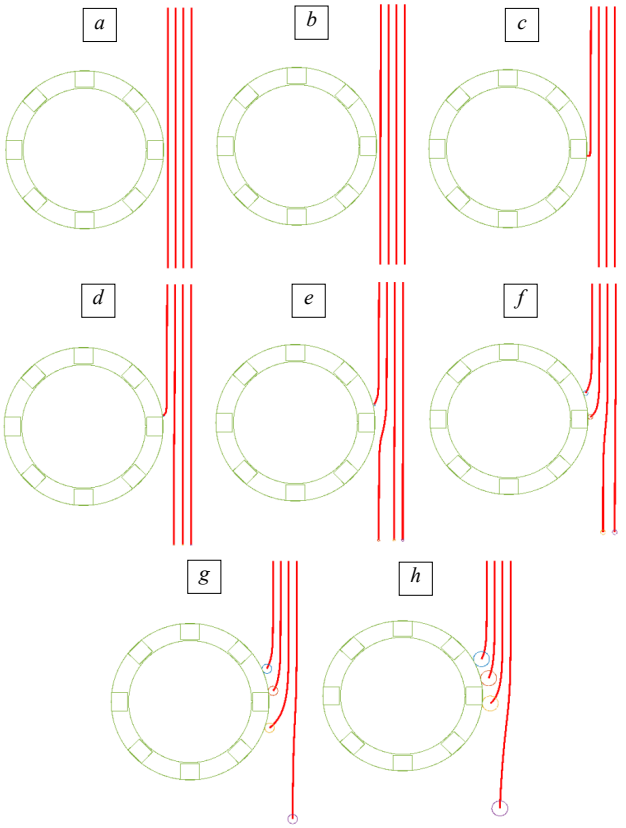

Fig. 8. Computed particle trajectories obtained in granular medium: *a*) D_p=70·10^{-6} m; *b*) D_p=150·10^{-6} m; *c*) D_p=300·10^{-6} m; *d*) D_p=800·10^{-6} m; *e*) D_p=1500·10^{-6} m; *f*) D_p=3000·10^{-6} m; *g*) D_p=6000·10^{-6} m; *h*) D_p=10000·10^{-6} m

The evaluation of the capture time of the separated particles has given the results listed in Table 3. It is clearly seen that the larger size particles are also captured faster.

Table 3

Capture time of separated particles in presence of the granular frictional drag force

Particle diameter D_p ($\times 10^{-6}$ m)	Particle capture time, s		
	1	2	3
70	–	–	–
150	–	–	–
300	0.1387	–	–
800	0.1290	–	–
1500	0.1251	–	–
3000	0.1204	0.1333	–
6000	0.1170	0.1283	0.1483
10000	0.1141	0.1248	0.1382

The computation of the particle trajectories and capture time for other packing fractions φ=0.21 and φ=0.61 has given almost the same findings.

The achieved theoretical study has shown that the frictional drag force has important effect on the separation efficiency. In granular ores of fine grains, such effect can dominate the magnetic force and may even prevent the separation.

Experimental verification. To validate the achieved theoretical study and verify the obtained results, experiments were carried out on mixtures of sand and iron particles of μ_r=115 experimentally identified. In order to reduce the effect of the magnetic dipole-dipole interaction that leads to particle agglomerations before their separation (case in which the frictional drag force will not be applied individually on the particles) [41], mixtures of weak concentrations of iron particles were considered.

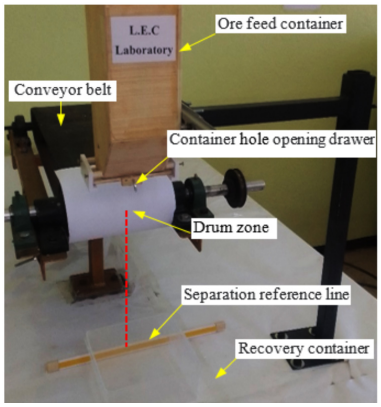

Fig. 9. Experimental used separator

The used OGMS separator is a permanent magnet (B_r=1.1 T) drum separator [16] equipped with a container allowing the feeding of the granular material by gravity instead of its transporting by conveyor belt (Fig. 9). In this way, the friction between the particles to be separated and the belt is entirely excluded, and only the friction with the sand grains is considered.

As we previously mentioned, the iron ore is crushed to small grains before proceeding to magnetic separation. Therefore, the experimental verification is limited to iron particles of diameter $D_p < 10^{-3}$ m. In order to reduce the study cost, ranges of particle diameters $D_p < 8{\cdot}10^{-5}$ m, $2{\cdot}10^{-4}$ m $< D_p < 4{\cdot}10^{-4}$ m and $6{\cdot}10^{-4}$ m $< D_p < 10^{-3}$ m experimentally identified are treated (Fig. 10).

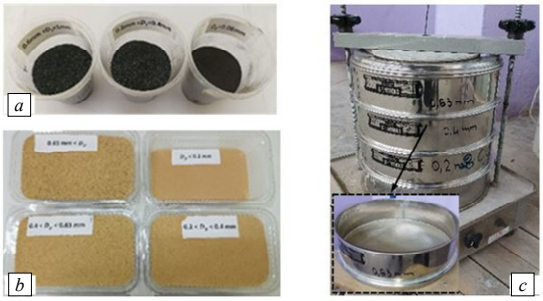

Fig. 10. *a* – identified ranges of magnetic particles; *b* – identified ranges of granular material grains; *c* – used sieving device

To verify the nature of dependence between the particle size and the separation efficiency theoretically obtained on one hand and to obtain basic results subsequently making it possible to distinguish possible effects of the granular drag force on the other hand, a first series of experiments have been performed without considering the granular medium. To permit a comparison between theoretical and experimental results, the same operating conditions must be considered. Accordingly, we have chosen a container orifice $w = 10^{-2}$ m, a lift-off $e = 3.4{\cdot}10^{-2}$ m and shifting distance $d = 2{\cdot}10^{-2}$ m, which gives a feeding limit $l = d+w = 3{\cdot}10^{-2}$ m from the drum surface (see Fig. 1).

The injection of a same volume $V_i = 10^{-6}$ m^3 of particles in the separator gave for the considered particle sizes the results presented in Fig. 11. The qualitative examination of the non-separated quantities (quantities circled in red «1») for each case shows that the larger the particle size, the greater the separated quantity (quantities circled in yellow «2»). Here, the particle is considered separated if it is captured by the drum or fallen behind the separation reference (see Fig.9).

In order to consolidate our verification, we quantified the separated volume of particles. Such quantification gave for the considered cases of particle size the results presented in Table 4. The latter confirms clearly the proportional relationship between the particle size and the separation efficiency found theoretically through a comparison of capture times (see Table 2).

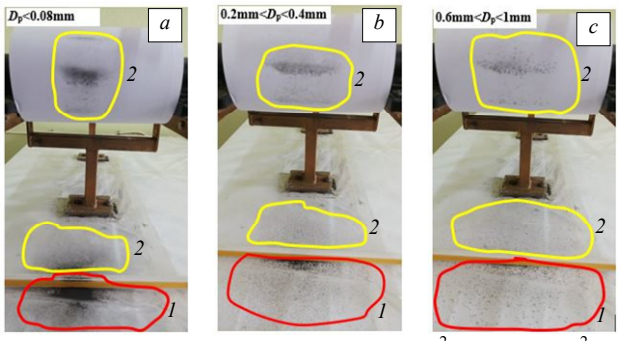

Fig. 11. Separated particles obtained for $w = 10^{-2}$ m, $e = 3.4{\cdot}10^{-2}$ m, $d = 2{\cdot}10^{-2}$ m without granular medium. The considered iron particle diameters are: *a*) $R_p < 8{\cdot}10^{-5}$ m; *b*) $2{\cdot}10^{-4}$ m $< R_p < 4{\cdot}10^{-4}$ m; *c*) $6{\cdot}10^{-4}$ m $< R_p < 10^{-3}$ m

Table 4

Separated volume of particles without considering the granular medium

Particle diameter D_p, m	Separated volume, m^3
$D_p < 8{\cdot}10^{-5}$	$176.1{\cdot}10^{-9}$
$2{\cdot}10^{-4} < D_p < 4{\cdot}10^{-4}$	$260.6{\cdot}10^{-9}$
$6{\cdot}10^{-4} < D_p < 10^{-3}$	$357.3{\cdot}10^{-9}$

To verify experimentally the use limits of separation without considering the granular medium, we quantified the separated volume of particles for different shifting distances d (see Fig.1). The obtained results for the considered particle sizes are presented in Table 5.

Table 5

Separated volume of particles (separation efficiency) without granular medium

Shifting distance d ($\times 10^{-2}$ m)	Separated volume V_s($\times 10^{-9}$ m^3)		
	D_p<$8{\cdot}10^{-5}$ m	$2{\cdot}10^{-4}$ m $< D_p$ $D_p < 4{\cdot}10^{-4}$ m	$6{\cdot}10^{-4}$ m $< D_p$ $D_p < 10^{-3}$ m
0	**990.8**	928.7	930.8
1	**770.5**	580.2	625
2	176.1	260.6	357.3
4	33.6	45.8	118.1
6	<9.2	<18.3	42.8
8	0	0	9.2
10	0	0	0

If we neglect the singular values written in bold, we also see a proportional relationship between the particle size and the separation efficiency. A significant separation is approximately obtained for a limit $y_0 \approx 6{\cdot}10^{-2}$ m, which is really greater than that found theoretically

$$y_0 = 1.25{\cdot}10^{-2} \text{ m}.$$

The difference between the experimental and computed values is mainly related to dipole-dipole interaction neglected in the theoretical study [41].

To estimate the effect of the frictional drag force on the separation efficiency, we treated samples of a mixture of sand and iron particles for different sizes of sand grains and particles. To obtain homogeneous dispersion of the particles in the sand, the mixture is well prepared.

To permit a comparison between the results related to each case of the composition size of the mixture, we always treated the same volume with same fractions of sand and iron particles. Practically, we inject in the separator, each time, a sample composed of a volume $V_s = 6{\cdot}10^{-4}$ m^3 of sand and a volume $V_i = 10^{-6}$ m^3 of iron particles.

For the same operating conditions of the drum and geometrical parameters $w = 10^{-2}$ m, $e = 3.4{\cdot}10^{-2}$ m and $d = 1.5{\cdot}10^{-2}$ m, the experiment effected with sand of grains size $D_g < 0.2{\cdot}10^{-3}$ m has given for the considered size

ranges of the iron particles the results of Fig. 12. In the latter, the separated particles are circled in yellow.

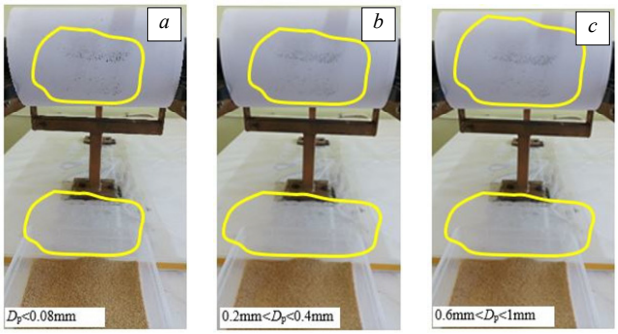

Fig. 12. Separated particles obtained for $w = 10^{-2}$ m, $e = 3.4 \cdot 10^{-2}$ m $d = 1.5 \cdot 10^{-2}$ m with granular medium (sand) of grains diameter $D_g < 0.2 \cdot 10^{-3}$ m. The considered iron particle diameters are: *a*) $R_p < 8 \cdot 10^{-5}$ m; *b*) $2 \cdot 10^{-4}$ m $< R_p < 4 \cdot 10^{-4}$ m; *c*) $6 \cdot 10^{-4}$ m $< R_p < 10^{-3}$ m

The qualitative comparison between Fig. 11 and Fig. 12 shows clearly that the separation efficiency degraded. The same findings have been found by experiments achieved with sand of grains sizes $2 \cdot 10^{-4}$ m $< D_g < 4 \cdot 10^{-4}$ m, $4 \cdot 10^{-4}$ m $< D_g < 6.3 \cdot 10^{-4}$ m and $D_g > 6.3 \cdot 10^{-4}$ m.

To estimate the degradation of separation efficiency, we quantified the separated volume of particles for the considered cases of particle size. The assembling, for each case, the particles captured by the drum and those fallen behind the separation line gave the results presented in Table 6. The latter shows that in presence of the granular medium, the separation efficiency always increases with the increase in the size of the iron particles.

Table 6

Separated volume of particles (separation efficiency) with granular medium

Sand grains diameter D_g	Separated volume $V_s(\times 10^{-9}$ m$^3)$		
	$D_p < 8 \cdot 10^{-5}$ m	$2 \cdot 10^{-4}$ m $< D_p$ $D_p < 4 \cdot 10^{-4}$ m	$6 \cdot 10^{-4}$ m $< D_p$ $D_p < 10^{-3}$ m
$D_g > 0.63 \cdot 10^{-3}$m	49.9	81.4	107.9
$0.4 \cdot 10^{-3}$ m $< D_g$ $D_g < 0.63 \cdot 10^{-3}$ m	18.3	68.2	**139.4**
$0.2 \cdot 10^{-3}$ m $< D_g$ $D_g < 0.4 \cdot 10^{-3}$ m	**28.5**	63.1	122.1
$D_g < 0.2 \cdot 10^{-3}$ m	<9.2	**49.9**	42.8

Looking at the results of Table 5 obtained for the same w and $d = 2 \cdot 10^{-2}$ m, we see that without granular medium the separation efficiency is very important in relation to that obtained in presence of the granular medium with a lower distance $d = 1.5 \cdot 10^{-2}$ m, which verifies clearly the important effect of the frictional drag force.

Another reading of the results of Table 6 shows that (apart from the singular values written in bold) for a given size of the iron particle, the separation efficiency degrades with the increase in the grains size of the sand.

To know the effect of the frictional drag force in relatively weak applied magnetic field, experiments was achieved for a larger container orifice $w = 3 \cdot 10^{-2}$ m. The results obtained for the same values of e and d are presented in Table 7. The latter shows that apart from the degradation of the separation efficiency due to the decreasing of the field, the proportionality between the particle size and the separation efficiency is lost.

Table 7

Separated volume of particles (separation efficiency) with granular medium, $w = 3 \cdot 10^{-2}$ m

Sand grains diameter D_g	Separated volume $V_s(\times 10^{-9}$ m$^3)$		
	$D_p < 8 \cdot 10^{-5}$ m	$2 \cdot 10^{-4}$ m $< D_p$ $D_p < 4 \cdot 10^{-4}$ m	$6 \cdot 10^{-4}$ m $< D_p$ $D_p < 10^{-3}$ m
$D_g > 0.63 \cdot 10^{-3}$ m	<<18.3	**45.8**	40.7
$0.4 \cdot 10^{-3}$ m $< D_g$ $D_g < 0.63 \cdot 10^{-3}$ m	<<18.3	34.6	21.4
$0.2 \cdot 10^{-3}$ m $< D_g$ $D_g < 0.4 \cdot 10^{-3}$ m	20.4	28.5	**27.5**
$D_g < 0.2 \cdot 10^{-3}$ m	<<18.3	9.2–18.3	**<<9.2**

Conclusions. In this work, the effect of the frictional drag force on the efficiency of OGMS in dry granular material is estimated and experimentally verified. To permit such estimation, we have computed the particle trajectories where the granular material is approached to complex fluid for which the frictional drag force is assumed similar to fluid drag force analytically modelled.

To verify the theoretically obtained findings, experiments were carried out on mixtures of sand and iron particles of small size. The choice of sand is justified by the fact that, on one hand the used analytical model for the frictional drag force is valid for this type of material, and on the other hand, the mixtures do not differ much from real iron ore.

The achieved experiments have approved the theoretically obtained findings. The differences between the computed and experimental values are mainly related to the dipole-dipole magnetic interaction neglected in the theoretical study. Practically, such effect leads to particle transient agglomerations, which encourages the separation.

The singular values in tables written in bold are mainly related to measure errors committed during the injection of the material through the container or the assembling of the separated particles.

Finally, it can be concluded that, if the size of the iron particles to be separated is very important compared to that of the grains forming the granular medium (magnetic purification of materials), the frictional drag force can be neglected. But in granular materials, where the iron particles are of the same size of the grains (case of enrichment of fine grinded ores of low concentration of iron particles), the frictional drag force must be taken into account in any designing study.

Conflict of interest. The authors declare that they have no conflicts of interest.

REFERENCES

1. Ku J., Wang K., Wang Q., Lei Z. Application of Magnetic Separation Technology in Resource Utilization and Environmental Treatment. *Separations*, 2024, vol. 11, no. 5, art. no. 130. doi: https://doi.org/10.3390/separations11050130.

2. Kukkala P.C., Kumar S., Nirala A., Khan M.A., Alkahtani M.Q., Islam S. Beneficiation of Low-Grade Hematite Iron Ore Fines by Magnetizing Roasting and Magnetic Separation. *ACS Omega*, 2024, vol. 9, no. 7, pp. 7634-7642. doi: https://doi.org/10.1021/acsomega.3c06802.

3. Fariss A.H.B., Bicalho W.C.S., Seixas L., Faustino L.M. Beneficiation of low-grade iron ore using a dry-roll magnetic separator and its modeling via artificial neural network. *Journal of Sustainable Metallurgy*, 2025, vol. 11, art. no. 529. doi: https://doi.org/10.1007/s40831-025-01030.

4. Xie S., Hu Z., Lu D., Zhao Y. Dry Permanent Magnetic Separator: Present Status and Future Prospects. *Minerals*, 2022, vol. 12, no. 10, art. no. 1251. doi: https://doi.org/10.3390/min12101251.

5. Jiu S., Zhao B., Yang C., Chen Y., Cheng F. High-Efficiency Iron Extraction from Low-Grade Siderite via a Conveyor Bed Magnetization Roasting–Magnetic Separation Process: Kinetics Research and Applications. *Materials*, 2022, vol. 15, no. 18, art. no. 6260. doi: https://doi.org/10.3390/ma15186260.

6. Wang X., Hu Y., Hao Y., Shen Z., Liang G., Zhang M. Simulation of Dynamic Particle Trapping and Accumulation in HGMS Based on FEM-CFD-DEM Coupling Approach. *Processes*, 2025, vol. 13, no. 8, art. no. 2391. doi: https://doi.org/10.3390/pr13082391.
7. Liu J., Dai H., Yu L., Wang C., Feng J., Li P., Xu S. Optimization of the Matrix in a Transverse-Field High-Gradient Magnetic Separator for an Improved Ilmenite Separation. *Minerals*, 2025, vol. 15, no. 2, art. no. 114. doi: https://doi.org/10.3390/min15020114.
8. Vilakazi A.Q., Shemi A., Ndlovu S. Dry Magnetic Separation and the Leaching Behaviour of Aluminium, Iron, Titanium, and Selected Rare Earth Elements (REEs) from Coal Fly Ash. *Minerals*, 2025, vol. 15, no. 2, art. no. 119. doi: https://doi.org/10.3390/min15020119.
9. Chokin K., Yedilbayev A., Yugai V., Medvedev A. Beneficiation of Magnetically Separated Iron-Containing Ore Waste. *Processes*, 2022, vol. 10, no. 11, art. no. 2212. doi: https://doi.org/10.3390/pr10112212.
10. Liu J., Xue Z., Dong Z., Yang X., Fu Y., Man X., Lu D. Multiphysics Modeling Simulation and Optimization of Aerodynamic Drum Magnetic Separator. *Minerals*, 2021, vol. 11, no. 7, art. no. 680. doi: https://doi.org/10.3390/min11070680.
11. Baawuah E., Kelsey C., Addai-Mensah J., Skinner W. A Novel Pneumatic Planar Magnetic Separator for Magnetite Beneficiation: A Focus on Flowsheet Configuration. *Minerals*, 2020, vol. 10, no. 9, art. no. 759. doi: https://doi.org/10.3390/min10090759.
12. Luukkanen S., Tanhua A., Zhang Z., Mollehuara Canales R., Auranen I. Towards waterless operations from mine to mill. *Minerals Engineering*, 2022, vol. 187, art. no. 107793. doi: https://doi.org/10.1016/j.mineng.2022.107793.
13. Yi F., Chen L., Liu X., Zeng J., Xue Z. Development of a centrifugal dry magnetic separator for separation of fine magnetite ore. *Powder Technology*, 2024, vol. 437, art. no. 119557. doi: https://doi.org/10.1016/j.powtec.2024.119557.
14. Lu D., Liu J., Cheng Z., Li X., Xue Z., Li S., Zheng X., Wang Y. Development of an open-gradient magnetic separator in the aerodynamic field. *Physicochemical Problems of Mineral Processing*, 2020, vol. 56, no. 2, pp. 325-337. doi: https://doi.org/10.37190/ppmp20005.
15. Li X., Wang Y., Lu D., Zheng X., Gao X. Optimization of Airflow Field for Pneumatic Drum Magnetic Separator to Improve the Separation Efficiency. *Minerals*, 2021, vol. 11, no. 11, art. no. 1228. doi: https://doi.org/10.3390/min11111228.
16. Ouili M., Mehasni R., Feliachi M., Belounis A., Latreche M.E.H. A simultaneous separation of magnetic and conductive particles in a designed permanent magnet drum separator. *International Journal of Applied Electromagnetics and Mechanics*, 2019, vol. 61, no. 1, pp. 137-155. doi: https://doi.org/10.3233/JAE-180101.
17. Zeng J., Tong X., Yi F., Chen L. Selective Capture of Magnetic Wires to Particles in High Gradient Magnetic Separation. *Minerals*, 2019, vol. 9, no. 9, art. no. 509. doi: https://doi.org/10.3390/min9090509.
18. Belounis A., Mehasni R., Ouili M., Latreche M.E. Optimization of the capture element for an OGMS based on the 3D computation of the magnetic particle behavior. *International Journal of Applied Electromagnetics and Mechanics*, 2015, vol. 48, no. 4, pp. 387-397. doi: https://doi.org/10.3233/JAE-140157.
19. Mehasni R., Latreche M., Feliachi M. Fine particles behavior analysis for magnetic separation process. *International Journal of Applied Electromagnetics and Mechanics*, 2004, vol. 19, no. 1–4, pp. 587-590. doi: https://doi.org/10.3233/JAE-2004-633.
20. Katsuragi H., Durian D.J. Drag force scaling for penetration into granular media. *Physical Review E*, 2013, vol. 87, no. 5, art. no. 052208. doi: https://doi.org/10.1103/PhysRevE.87.052208.
21. Ye X., Wang D., Zhang X., Zhang C., Du W., Su X., Li G. Projectile oblique impact on granular media: penetration depth and dynamic process. *Granular Matter*, 2021, vol. 23, no. 2, art. no. 48. doi: https://doi.org/10.1007/s10035-021-01108-3.
22. Omidvar M., Iskander M., Bless S. Response of granular media to rapid penetration. *International Journal of Impact Engineering*, 2014, vol. 66, pp. 60-82. doi: https://doi.org/10.1016/j.ijimpeng.2013.12.004.
23. Pol A., Storti S., Gabrieli F. Granular drag and lift force on a flexible fiber. *Physical Review E*, 2025, vol. 112, no. 4, art. no. 045425. doi: https://doi.org/10.1103/p2db-yt7h.
24. Brzinski T.A., Mayor P., Durian D.J. Depth-Dependent Resistance of Granular Media to Vertical Penetration. *Physical Review Letters*, 2013, vol. 111, no. 16, art. no. 168002. doi: https://doi.org/10.1103/PhysRevLett.111.168002.
25. Marghitu D., Lee S., Marghitu D. Experimental and Simulation Results for the Impact of a Rotating Flexible Link with a Granular Material. *International Journal of Advanced Robotic Systems*, 2014, vol. 11, no. 1, art. no. 40. doi: https://doi.org/10.5772/58254.
26. Zhang C., Ye X. Force and flow characteristics of an intruder immersed in 3D dense granular matter. *Particuology*, 2022, vol. 71, pp. 47-55. doi: https://doi.org/10.1016/j.partic.2022.01.007.
27. Katsuragi H., Durian D.J. Unified force law for granular impact cratering. *Nature Physics*, 2007, vol. 3, no. 6, pp. 420-423. doi: https://doi.org/10.1038/nphys583.
28. Wang F., Chen Y., Li Y., Li Y. A Drag Force Model of Vertical Penetration into a Granular Medium Based on DEM Simulations and Experiments. *Applied Sciences*, 2024, vol. 14, no. 6, art. no. 2336. doi: https://doi.org/10.3390/app14062336.
29. Zaidi A.A. Numerical investigation of drag force on a spherical intruder by granular material. *Powder Technology*, 2023, vol. 427, art. no. 118765. doi: https://doi.org/10.1016/j.powtec.2023.118765.
30. Dodds D., Sarhan A.R., Naser J. Experimental and numerical study of drag forces on particles in clusters. *Powder Technology*, 2020, vol. 371, pp. 195-208. doi: https://doi.org/10.1016/j.powtec.2020.05.082.
31. Zaidi A.A. Granular drag force during immersion in dry quicksand. *Powder Technology*, 2020, vol. 364, pp. 986-993. doi: https://doi.org/10.1016/j.powtec.2019.10.048.
32. Lavinsky D.V., Zaitsev Y.I. Computational studies of electromagnetic field propagation and deforming of structural elements for a thin-walled curved workpiece and an inductor. *Electrical Engineering & Electromechanics*, 2024, no. 2, pp. 55-60. doi: https://doi.org/10.20998/2074-272X.2024.2.08.
33. Gans Š., Molnár J., Kováč D. Estimation of electrical resistivity of conductive materials of random shapes. *Electrical Engineering & Electromechanics*, 2023, no. 6, pp. 72-76. doi: https://doi.org/10.20998/2074-272X.2023.6.13.
34. Ouili M., Mehasni R., Feliachi M., Latreche M.E.H. Coupling of PSO and FE methods for electrical conductivity identification of materials used in eddy current separator. *International Journal of Applied Electromagnetics and Mechanics*, 2023, vol. 72, no. 2, pp. 103-114. doi: https://doi.org/10.3233/JAE-220248.
35. Yang Y., Robertson W.S.P., Jafari A., Arjomandi M. Advanced Numerical Approaches for Magnetic Force Calculations: A Comprehensive Review. *Progress In Electromagnetics Research B*, 2025, vol. 115, pp. 78-94. doi: https://doi.org/10.2528/PIERB25071902.
36. Bastos J.P.A., Sadowski N. *Electromagnetic Modeling by Finite Element Methods*. CRC Press, 2003. 510 p. doi: https://doi.org/10.1201/9780203911174.
37. Tolmachev S.T., Bondarevskyi S.L., Il'chenko A.V. Magnetic properties of multicomponent heterogeneous media with a doubly periodic structure. *Electrical Engineering & Electromechanics*, 2020, no. 1, pp. 29-38. doi: https://doi.org/10.20998/2074-272X.2020.1.05.
38. Milykh V.I., Tymin M.G. A comparative analysis of the parameters of a rotating magnetic field inductor when using concentric and loop windings. *Electrical Engineering & Electromechanics*, 2021, no. 4, pp. 12-18. doi: https://doi.org/10.20998/2074-272X.2021.4.02.
39. Grechko O.M. Influence of the poles shape of DC electromagnetic actuator on its thrust characteristic. *Technical Electrodynamics*, 2024, no. 1, pp. 38-45. doi: https://doi.org/10.15407/techned2024.01.038.
40. Lohse D., Rauhe R., Bergmann R., Van der Meer D. Creating a dry variety of quicksand. *Nature*, 2004, vol. 432, no. 7018, pp. 689-690. doi: https://doi.org/10.1038/432689a.
41. Mehasni R., Feliachi M., Latreche M.E.H. Effect of the Magnetic Dipole–Dipole Interaction on the Capture Efficiency in Open Gradient Magnetic Separation. *IEEE Transactions on Magnetics*, 2007, vol. 43, no. 8, pp. 3488-3493. doi: https://doi.org/10.1109/TMAG.2007.897616.

Received 20.10.2025
Accepted 27.12.2025
Published 02.05.2026

O. Belguet[1], *PhD,*
R. Mehasni[1], *Professor,*
A. Belounis[2], *Doctor of Electrical Engineering,*
M. Ouili[1], *Doctor of Electrical Engineering,*
[1] Electrical Laboratory of Constantine (LEC),
Constantine 1 University, Algeria,
e-mail: oussama.belguet@lec-umc.org (Corresponding Author).
[2] 20th August 1955 University, Algeria.

How to cite this article:
Belguet O., Mehasni R., Belounis A., Ouili M. Effects of friction on the efficiency of open gradient magnetic separation in dry granular materials. *Electrical Engineering & Electromechanics*, 2026, no. 3, pp. 3-10. doi: https://doi.org/10.20998/2074-272X.2026.3.01